JOURNAL OF SOLID STATE CHEMISTRY 74, 74–87 (1988)

Macro- and Microstructural Analysis of $R Ba_2Cu_3O_{7-x}$ (R = Y, Gd, Er, and Tm) Superconductor Thin Crystals between 300 and 15 K

M. GASGNIER

ER 210, CNRS Bellevue, 1 Place A. Briand, 92195 Meudon Cedex, France

M.-O. RUALT

Centre de Spectrométrie Nucléaire et de Spectrométrie de Masse, CNRS, Bat. 108, 91406 Orsay Cedex, France

P. TREMBLAY

Laboratoire de Géochimie des roches sédimentaires, UA 723 CNRS, Bat. 504, Université Paris-Sud, 91405, Orsay Cedex, France

AND P. GOUGEON, M. POTEL, J. C. LEVET, AND H. NOEL

Laboratoire de Chimie Minérale B, LA 254, Université de Rennes I, Campus de Beaulieu, 35042 Rennes Cedex, France

Received July 21, 1987; in revised form October 30, 1987

Some macro- and microstructural crystallographic properties of the new superconductors $R Ba_2 Cu_3O_{7-x}$ (R = Y, Gd, Er, Tm) have been studied. Chemical composition of some uncrushed monocrystalline $ErBa_2Cu_3O_{7-x}$ have been determined by scanning electron microscopy fitted to an energy dispersive X-ray spectrometer. Conventional transmission electron microscopy with a liquid He cooled stage showed that only ~25% of small crushed crystals have defected zones as dislocations or planar defects. Electron diffraction patterns point out the presence of the orthorhombic and sometimes of the tetragonal structures of $YBa_2Cu_3O_{7-x}$. Other patterns show the presence of various known compounds (i.e., $BaCuO_2$) and unknown compounds often in coexistence with the well-established orthorhombic $R Ba_2Cu_3O_{7-x}$. © 1988 Academic Press, Inc.

Introduction

Since the recent discovery (*1, 2*) of the new generation of superconductor materials $R Ba_2Cu_3O_{7-x}$ (R = rare earth) many results have been reported. In the field of microstructural characterizations, conventional transmission electron microscopy (CTEM) and high-resolution electron microscopy (HREM) were used essentially to determine the intrinsic properties of the orthorhombic and tetragonal structures of the well-defined compound (*3–12*). Over- or substoichiometric oxygen compositions (*13, 14*) and rich or deficient rare earth contents (*15*) were also studied. One must no-

0022-4596/88 $3.00

tice that (i) studied materials present mostly a high density of twins and oriented domains, (ii) there is a coexistence, with the superconductor compound, of various chemical compounds: R_2O_3, $BaCuO_2$, $R_2Cu_2O_5$, and pseudoternary systems. From X-ray diffraction techniques Quadri *et al.* (*16*) and Tarascon *et al.* (*17*) have reported that numerous diffraction peaks are not in agreement with well-defined structures. However, electron and X-ray diffraction led to new crystalline structures which are generally orthorhombic or tetragonal (*6, 11, 14–17*).

The aim of this paper is to study the crystallographic properties of different RBa$_2$Cu$_3$O$_{7-x}$ compounds (R = Y, Gd, Er, and Tm) in relation to one another and also to compare the results reported elsewhere. The more important observations have been done in CTEM supplied with a liquid He-cooled sample holder (*18*) as reported in our initial results (*19*). Complementary results based on X-ray dispersive spectrometry (EDX), scanning electron microscopy (SEM), and X-ray diffraction are also reported here.

Experimental Methods

The purity of materials used for the RBa$_2$Cu$_3$O$_{7-x}$ crystal preparation was 99.9%. The crystals were prepared under air and annealed under an oxygen flow at 800 K for ~12 hr (*20*). The T_c, measured by Meissner effect, is close to 90 K. They are black and consist of small single-crystal aggregates overlapping one another. Their "bulk" configuration and chemical composition have been studied by SEM on a Philips 505 fitted with an X-ray dispersive spectrometer (EDX-Link System AN 10000). The program used is a ZAF 4FLS with virtual standards (VSP) corrected in relation to our apparatus.

In order to study these materials by electron microscopy, the small crystals were crushed with an agate mortar and the fine powder mixed with carbon tetrachloride. The bath was stirred to deposit the lighter particles on copper grids overlayed by a thin carbon film. The observations are mostly performed with a Philips EM400 (120 kV) supplied with a side-entry liquid He cooled stage. This device permits us to cool down the samples from room temperature to 10–15 K in a short time (~15 min). To avoid contamination, the vacuum around the sample was kept at values below 7×10^{-5} Pa, and an annular liquid nitrogen-cooled anticontamination device surrounded the sample. With this system it is also relatively easy to stabilize the temperature around 90–100 K during sample warming. The point-to-point resolution is about 2.5–3 nm (*18*). The samples can be heated by means of the focused electron beam. Electron diffraction patterns (EDP) provide crystallographic results with an accuracy of ~2%. Until now, to our knowledge only Ourmazd *et al.* (*3*) have performed low-temperature electron microscopy observations (40–270 K) on these superconducting materials. Other authors (*10*) propose future experiments.

Macrostructural Results

(*i*) *X-Ray Diffraction Patterns*

The finest particles of the uncrushed powder were studied by X-ray diffraction technique (Debye–Sherrer camera). According to uncrushed and crushed materials, the X-ray diffraction patterns reveal some differences:

—Only the orthorhombic structure is present for both uncrushed and crushed gadolinium compound (as in Fig. 1a). The diffraction-peak intensities are close to those reported by Reller *et al.* (*8*).

—Uncrushed yttrium compound is well represented by the classical orthorhombic structure (Fig. 1a). After

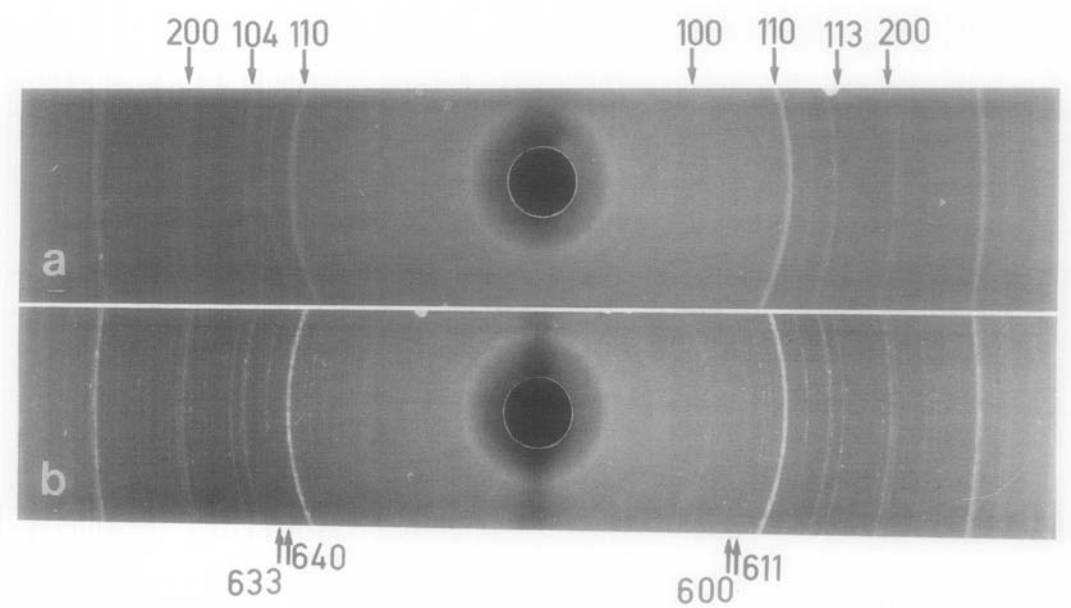

FIG. 1. (a) Typical XDP relative to the classical orthorhombic structure, i.e., pattern obtained from uncrushed $YBa_2Cu_3O_{7-x}$ material; (b) XDP of the same material after crushing. In addition to the orthorhombic structure, new diffraction peaks relative to the $BaCuO_2$ compound appear clearly. Some of the peaks relative to $BaCuO_2$ are indexed on the pattern.

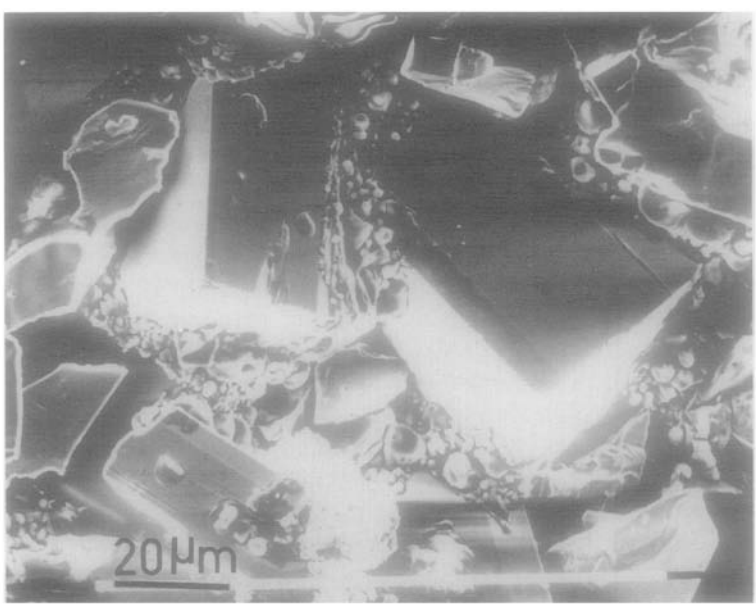

FIG. 2. Scanning electron microscopy of $YBa_2Cu_3O_{7-x}$ crystals.

crushing, X-ray diffraction patterns show the presence of additional peaks due to the $BaCuO_2$ (*bcc*, a = 1.826 nm) (Fig. 1b).

—In the case of erbium the patterns show the coexistence of the orthorhombic structure and the $BaCuO_2$ structure for both uncrushed and crushed material.

(ii) SEM and EDX Experiments

An overview of the initial material $ErBa_2Cu_3O_{7-x}$, shown in Fig. 2., is constituted by a small parallelepipedic-crystal intergrowth; their chemical composition can vary from one crystal to the other. Within some of these crystals, small isolated particles (inclusions) revealed by black contrast areas can be observed. Their chemical analysis revealed the lack of erbium within their volume. In the case of yttrium compound, the lack of $BaCuO_2$ diffraction peaks for uncrushed material is not yet clearly understood. One possible explanation is that small epitaxial $BaCuO_2$ particles are embedded in the matrix (as shown above), which are dissociated from the superconductor material in the course of the crushing.

To build a chemical map of the uncrushed crystals, one of them (Fig. 2) has been analyzed point by point according to a well-defined chequering (Fig. 3). Although many EDX analyses have been reported (*11*), no detailed chemical composition change on *one crystal* has been reported. The EDX quantitative analysis is done on a volume ~5 μ^3 with an accuracy better than 5%. Results are standardized to 100%. The oxides CuO, BaO, and Er_2O_3 were used for calibration. In this way 93 measurements were performed on crystal A. Five from crystal A and one from crystal B have been selected to show the relative fluctuations of the cationic elements for different zones (Table I and Fig. 3). The basic compound has the following formula: $Er_2Ba_4Cu_6O_{13}$. Some errors are due to the experimental method: (i) The crystals are not ideally planar and smooth, they can be slightly misoriented with regard to the detector window. (ii) There is another error on the copper and erbium contents due to the fact that the Cu(K) and Er(L) absorption edges have near equivalent energy values which require deconvolution calculations. (iii) There is a selective absorption effect for the lower energy, that is, the case of Ba(L) ab-

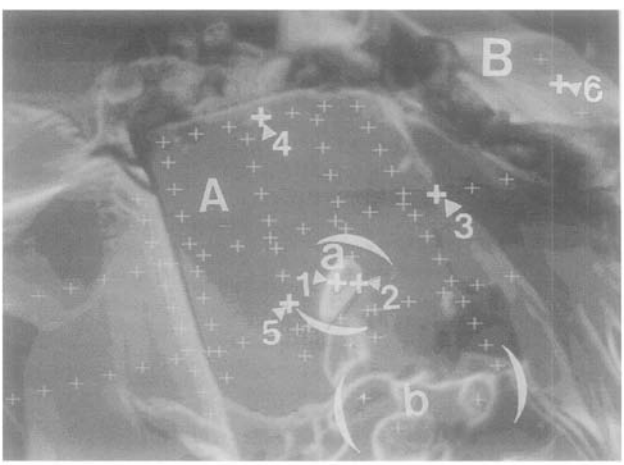

FIG. 3. SEM of $ErBa_2Cu_3O_{7-x}$ crystals showing the 93 points used to check the chemical content by means of energy dispersive X-ray spectrometry: five analyses are reported in Table I for crystal A (cross 1 to 5) and one for crystal B (cross 6).

TABLE I

CHEMICAL ANALYSIS OF DIFFERENT POINTS (1 TO 6) SHOWN IN FIG. 3

ELMT	ZAF	%ELMT	AT%		%Oxide	Formula
			Crystal A[a]			
			1: Cu very deficient			
CuK : O	1.172	13.205	13.800	Cu101	16.530	3.259
BaL : O	1.001	22.669	10.960	Ba101	25.310	2.588
ErL : O	.854	50.861	20.192	Er203	58.159	4.769
O K : O	.000	13.264	55.048			13.000
TOTAL		99.999	100.000		99.999	10.616
			2: Cu deficient			
CuK : O	1.124	24.895	23.289	Cu101	31.164	5.778
BaL : O	.977	34.043	14.734	Ba101	38.009	3.656
ErL : O	.818	26.959	9.581	Er203	30.827	2.377
O K : O	.000	14.103	52.395			13.000
TOTAL		100.000	100.000		100.000	11.811
			3: Cu normal			
CuK : O	1.119	25.814	23.953	Cu101	32.314	5.987
BaL : O	.976	37.303	16.014	Ba101	41.648	4.003
ErL : O	.815	22.770	8.027	Er203	26.038	2.006
O K : O	.000	14.113	52.007			13.000
TOTAL		100.000	100.000		100.000	11.997
			4: Cu excess			
CuK : O	1.115	27.200	24.930	Cu101	34.049	6.227
BaL : O	.972	34.995	14.839	Ba101	39.072	3.707
ErL : O	.812	23.506	8.184	Er203	26.878	2.044
O K : O	.000	14.299	52.046			13.000
TOTAL		100.000	100.000		100.000	11.978
			5: Cu large excess			
CuK : O	1.108	29.945	26.797	Cu101	37.486	6.691
BaL : O	.966	31.090	12.871	Ba101	34.712	3.214
ErL : O	.808	24.313	8.265	Er203	27.802	2.064
O K : O	.000	14.651	52.066			13.00
TOTAL		100.000	100.000		100.000	11.968
			6: Crystal B			
CuK : O	1.120	25.534	23.752	Cu101	31.963	5.939
BaL : O	.976	37.841	16.286	Ba101	42.250	4.072
ErL : O	.815	22.551	7.969	Er203	25.787	1.993
O K : O	.000	14.074	51.992			13.000
TOTAL		100.000	100.000		100.000	12.004

Absolute error = $\frac{\text{cation content} \times \text{Weight \% error}}{\text{Apparent concentration}}$

cation	error %
Cu	0.17
Ba	0.05
Er	0.09

[a] Absolute error = (cation content × weight % error)/apparent concentration. The cations and error % are respectively Cu, 0.17; Ba, 0.05; and Er, 0.09.

sorption edge. This sometimes leads to a slowly deficient barium content. However from the whole results and after aberrant analysis elimination (determined from the recorded-spectra background) it is possible to conclude that the main composition of the crystals is very close to the defined classical composition. The absolute errors for

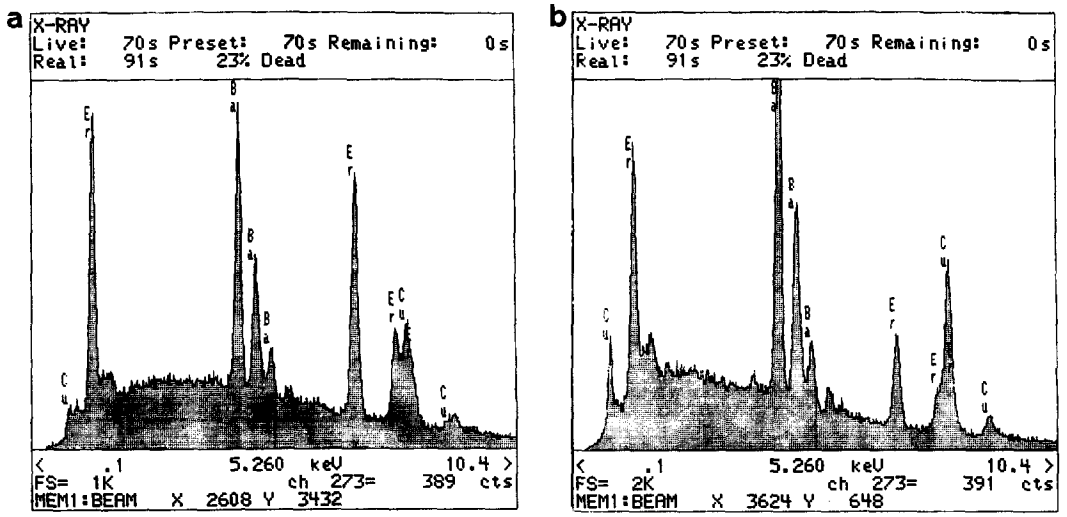

FIG. 4. Relative intensities of the Er(L), Ba(L), and Cu(K) absorption edges recorded by EDX. They show the content variation of three elements for two different crystal areas: (a) Zone (a) from crystal A (Fig. 3); (b) zone (6) from crystal B (Fig. 3).

the three cationic components are reported in Table I. Moreover one must notice that two zones of crystal A (indicated as zones (a) and (b)) are different in comparison to the other ones. Zone (a) is characterized by a bright contrast near the center, that

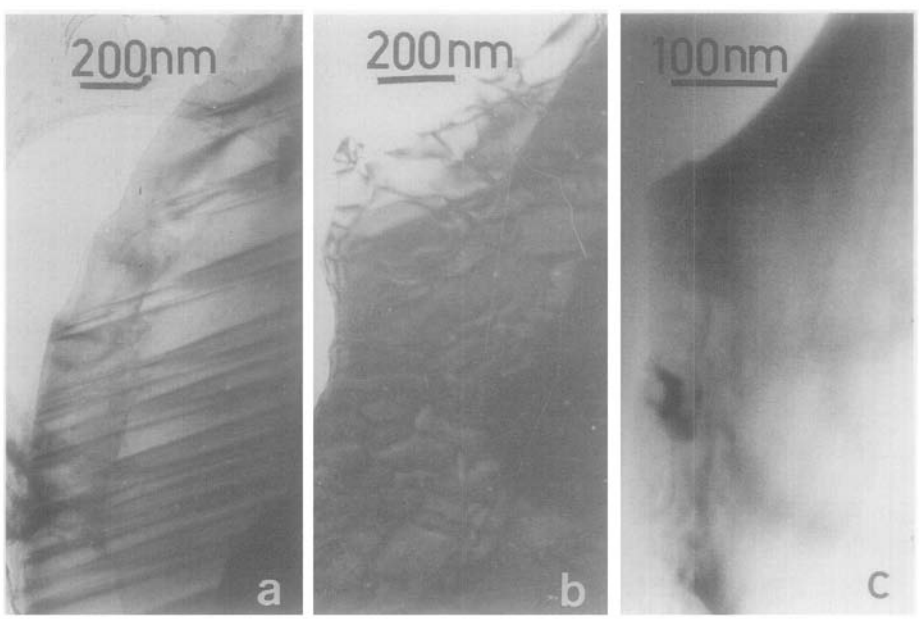

FIG. 5. CTEM: Bright fields (a) on a $YBa_2Cu_3O_{7-x}$ crystal at ~80 K showing stacking faults, (b) on a $YBa_2Cu_3O_{7-x}$ after warming from 15 to ~300 K showing dislocations, (c) on a $GdBa_2Cu_3O_{7-x}$ crystal at 300 K; this feature of a quasi-perfect crystal is mostly representative of the observed crystals (~75%).

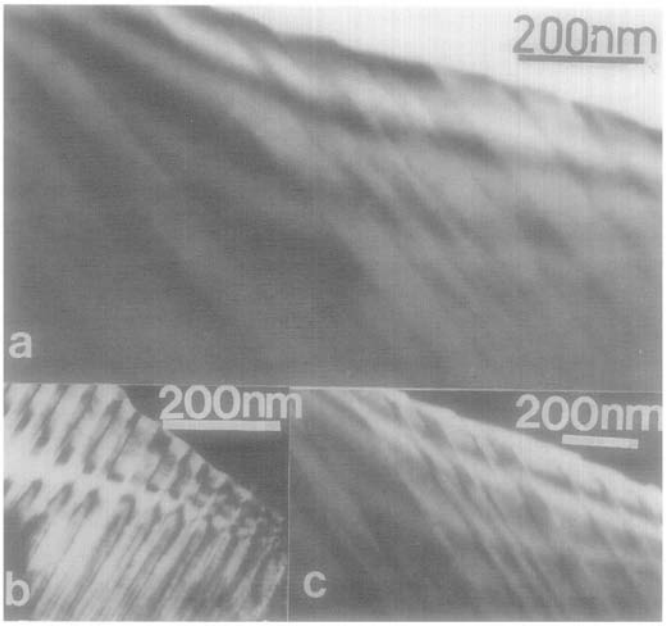

FIG. 6. CTEM on a $YBa_2Cu_3O_{7-x}$ crystal. (a) Bright field taken at 15 K showing planar defects. (b) Dark field of neighboring area taken after warming from 15 to 300 K. (c) Dark field of the same area at 15 K.

shows a copper and barium deficit with an erbium excess and a copper and erbium enrichment with a barium deficit around this zone. Zone (b) at the back central part is characterized by a copper and barium deficit with an erbium excess. EDX spectra reveal such composition variation, as shown in Figs. 4a and 4b, where relative intensities for Er, Ba, and Cu absorption edges are different according to the zones analyzed.

Microstructural Results

(*i*) *Observed Images*

Generally the observed microcrystals did not reveal any crystalline defects (as shown in Fig. 5c). Only ~25% of the crystals show crystalline defects as dislocations (Fig. 5b), planar defects, i.e., stacking faults (Fig. 5a), or microtwins in one direction (Fig. 6) or two perpendicular directions (Fig. 7). We can observe the characteristic contrasts of these planar defects on bright and dark fields (Figs. 6 and 7). From 15 K to room temperature a videorecording detected no change in the planar defect contrasts of the $YBa_2Cu_3O_{7-x}$ crystals, and they are even not sensitive to the electron beam of the microscope. Further analyses are in progress.

Our observations of relatively few planar defects are divergent with the results reported by Hervieu *et al.* (*9, 13*) and the presence of these planar defects obviously cannot explain the superconducting properties of these compounds. Similar conclusions were reported by Marks *et al.* (*12*) and Hyde *et al.* (*5*).

(*ii*) *Electron Diffraction Patterns*

Four different varieties of EDP were observed. Some possess very peculiar characteristics which are not clearly understood.

(a) For the three compounds (R = Y, Gd, Tm) over a range in (300–15 K), the patterns in general can be indexed according to

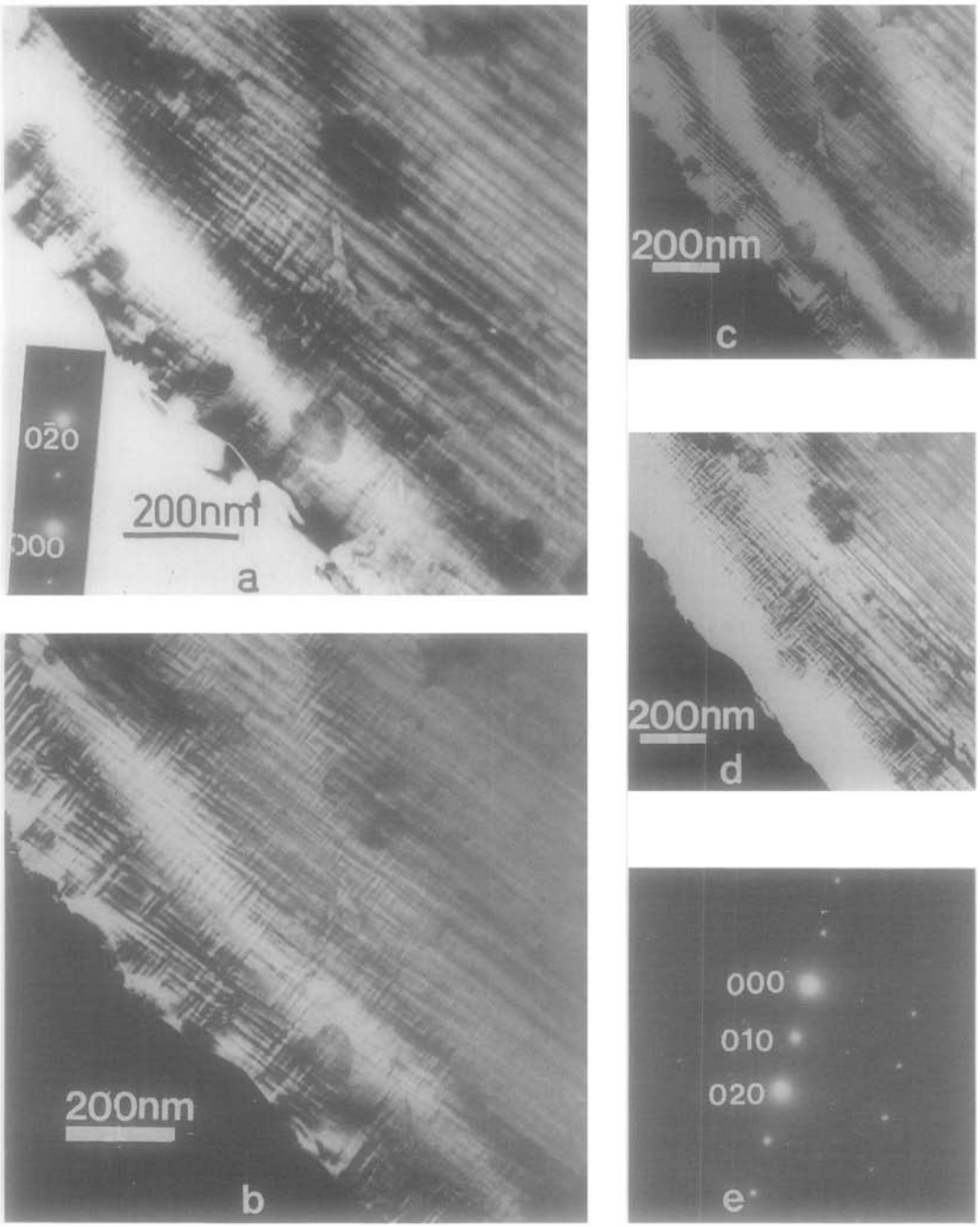

FIG. 7. CTEM on a $YBa_2Cu_3O_{7-x}$ crystal area after warming from 15 to 300 K showing microtwins. (a) Bright field: $g_{0\bar{2}0}$. (b–d) Dark fields with respectively $g_{0\bar{2}0}$, g_{020}, g_{010}. (e) Corresponding diffraction pattern.

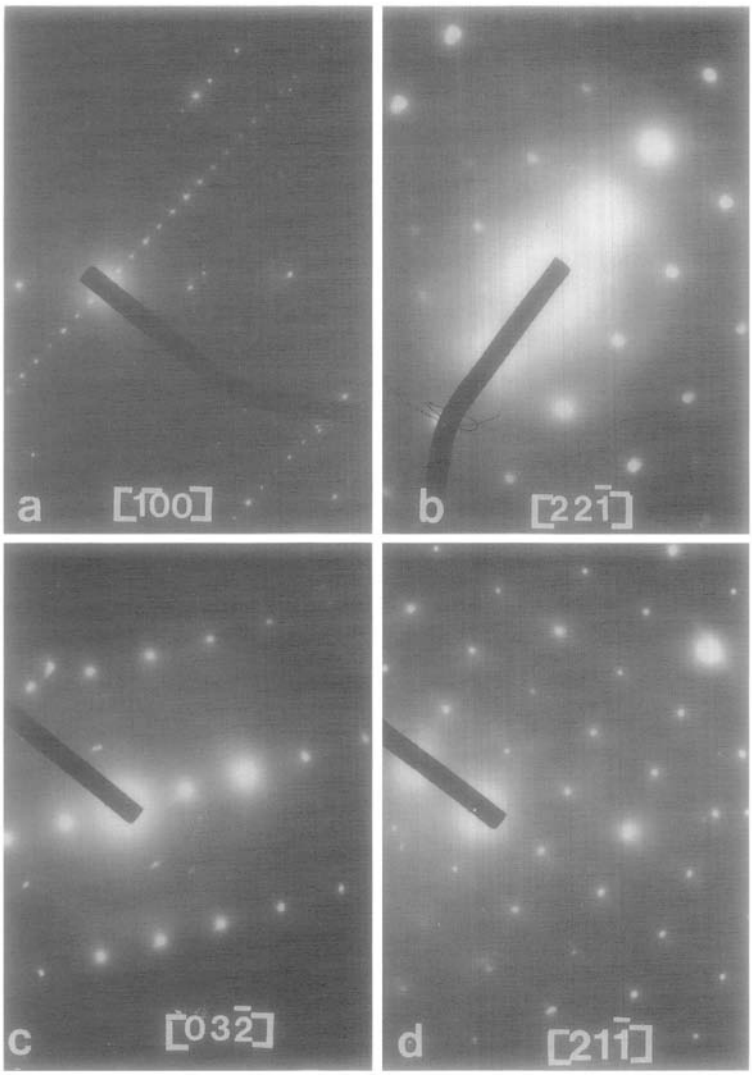

FIG. 8. Electron diffraction patterns of different areas relative to the orthorhombic structure. (a) $GdBa_2Cu_3O_{7-x}$ (15 K), zone axis [100]; (b) $TmBa_2Cu_3O_{7-x}$ (300 K), zone axis [22$\bar{1}$]; (c) $GdBa_2Cu_3O_{7-x}$ (15 K), zone axis [03$\bar{2}$]; (d) $GdBa_2Cu_3O_{7-x}$ (15 K), zone axis [21$\bar{1}$].

the classical orthorhombic structure (O_s). Their cell parameters are similar and nearly equal to the ones reported for $YBa_2Cu_3O_{7-x}$ (a = 0.382, b = 0.389, and c = 1.168 nm) (*11*). Among the large lot of diffraction patterns indexed, we have chosen some less classical zone axes (Fig. 8), and one with Kikuchi lines (Fig. 9).

Temperature variations of the sample lead to shifts in the position of the sample. Then, after a rapid sample cooling it is very difficult to unambiguously recognize at low temperature the microcrystals observed at room temperature due to a drastic shift in position. During warming, the temperature variations are slow and the sample-shift magnitudes are much smaller. So, the EDP videorecording was made during warming.

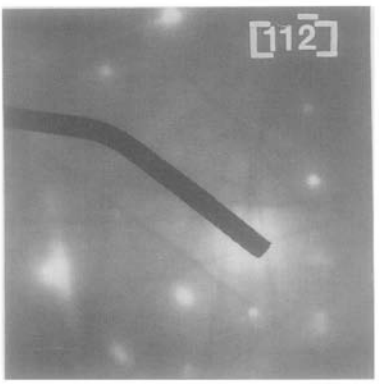

FIG. 9. EDP showing Kikuchi lines relative to a $YBa_2Cu_3O_{7-x}$ thicker crystal after warming from 15 to 300 K, zone axis [11$\bar{2}$].

However it is not always easy to visualize on the screen faint modification of the diffraction spot distances and/or positions and if such modifications can be observed, it is very tricky to determine the exact areas where they take place. In the case of $YBa_2Cu_3O_{7-x}$ crystals the orthorhombic (O_s) and the tetragonal ((T_s), with $a = 0.385$ and $c = 1.070$ nm) structures were observed after cooling at 15 K. The pattern sequence (Fig. 10) shows that the two structures are either well separated or in coexistence (*10*). Then the problem of the orthorhombic (O_s)–tetragonal (T_s) low-temperature transition has not been clearly resolved. Ourmazd *et al.* (*3*) do not observe this transition during cooling to 40 K. In contrast, this transition is well known at high temperature (between 850 and 1100 K (*15, 21, 22*). This phase transition is mostly due to an oxygen deficiency in the superconducting material, and the tetragonal structure was defined as $YBa_2Cu_3O_{6+y}$. In our case the small (T_s) crystal areas could be formed during the material preparation at 900 K. To try to observe the crystalline evolution toward high temperature, the crystals were annealed by means of the focused electron beam. However the small crystals either burst or become as small droplets (melt) too thick to be studied by electron diffraction (*19*).

(b) The next two classes have been reported in order to draw attention to some unexpected patterns. One only must indicate that the basic interplanar distances can always be indexed according to the orthorhombic structure (O_s). They are not

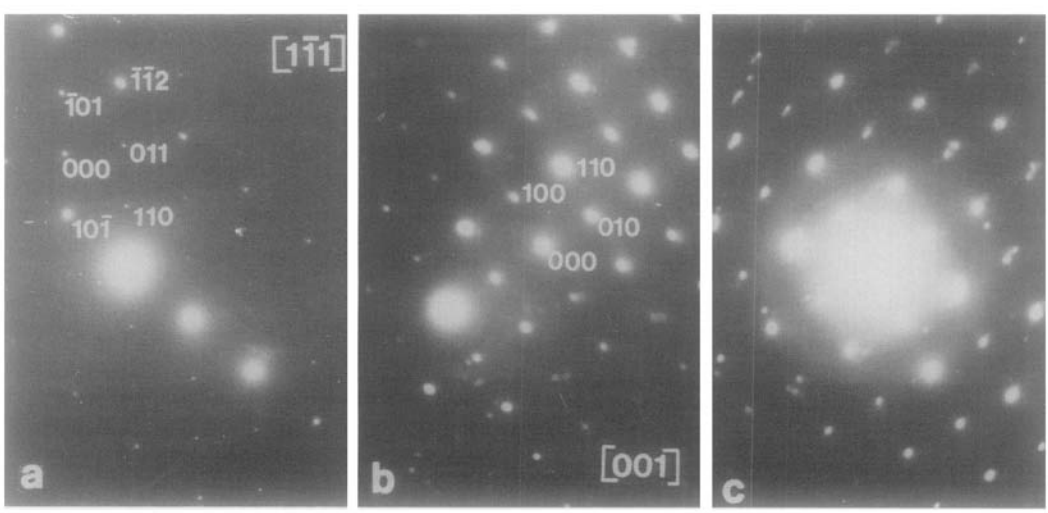

FIG. 10. EDP of $YBa_2Cu_3O_{7-x}$ crystals: (a) classical orthorhombic structure (300 K); (b) tetragonal structure (15 K); (c) coexistence of orthorhombic and tetragonal phases (15 K).

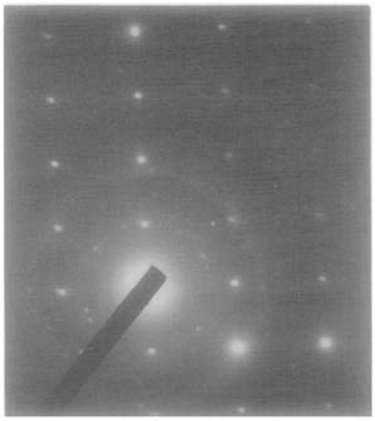

FIG. 11. "Asymmetrical" pattern relative to $TmBa_2Cu_3O_{7-x}$ (10 K). By comparison to the central row spots (indexed according to the $\{h00\}$ planes of the orthorhombic structure) the two nearest row spots are not exactly equidistant. Therefore the exact indexation becomes impossible.

easily interpreted as such situations are not classical and are difficult to describe in detail. The second class corresponds to asymmetrical EDP; i.e., the spot rows on both sides of the central one are not equidistant (Fig. 11). The third class is determined by unaligned row spot with an appearance of broken lines (Fig. 12).

(c) The last class of patterns concerns other compounds observed as isolated crystals. One of the most common is the compound $BaCuO_2$ (Figs. 13a and 13b). Its presence is not surprising and by comparison to XDP results we note that this compound was not observed for the $GdBa_2Cu_3O_{7-x}$ crystals. Some studies were performed on the $BaCuO_2$ phase stability against crystal temperature. The first results show that some crystals appear unstable. After cooling to 15 K, the EDP remained clearly indexable relative to the *bcc* cell (a = 1.826 nm). But, on warming at about 40 K, the patterns become unclear with spot systems doubled and even tripled. This permits us to calculate a larger *bcc* lattice (a = 1.935 nm). This phenomenon disappears at about 150 k. Other experiments will be done to clarify such a surprising situation.

No other compounds as Y_2O_3, $Y_2Cu_2O_5$, BaO, or CuO were detected. The other chemical compounds observed by electron microscopy seem to be consistent with

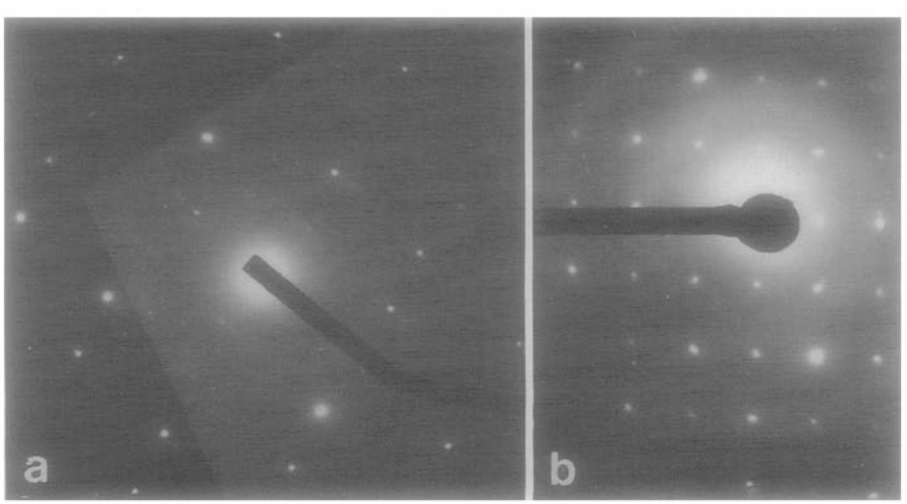

FIG. 12. EDP showing unaligned spots: the raws appeared to be as "broken lines"; (a) $TmBa_2Cu_3O_{7-x}$ (300 K); (b) $GdBa_2Cu_3O_{7-x}$ (300 K). Such patterns cannot be indexed.

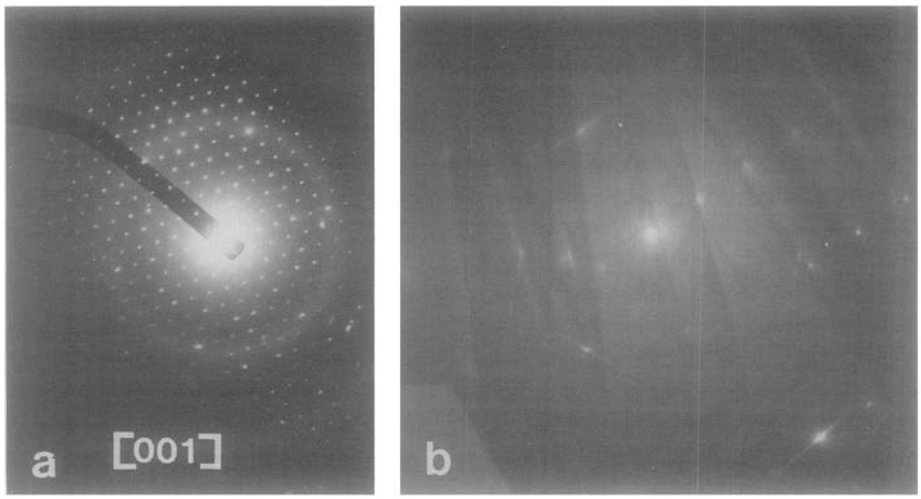

FIG. 13. EDP relative to $BaCuO_2$ (a) at 300 K, small crystal with a [001] zone axis (from $TmBa_2Cu_3O_{7-x}$ compound); (b) after warming from 15 to 300 K, small crystal with Kikuchi lines (from $YBa_2Cu_3O_{7-x}$ compound).

$R_xBa_yCu_zO_t$ ternary or pseudo-ternary systems (*6, 14–16*). One of them was indexed according to the orthorhombic structure of Gd_2BaCuO_5 (a = 1.220, b = 0.714, and c = 0.561 nm (*6, 14*)) as shown in Fig. 14. The two others, with unknown chemical content, are observed at 300 K in coexistence with $YBa_2Cu_3O_{7-x}$. The first gives another tetragonal cell (a = 0.365 and c = 1.985 nm) (Figs. 15a and 15b) and the second, a primitive cubic lattice cell (a = 0.645 nm). Their interreticular distances (d_{hkl}) are reported in Table II. One must notice that most of them are close to those of the (O_s) structure. Peculiarly the d_{100} of the new tetragonal cell and the d_{111} of the cubic one are close to the d_{101} or d_{011} of the (O_s) lattice.

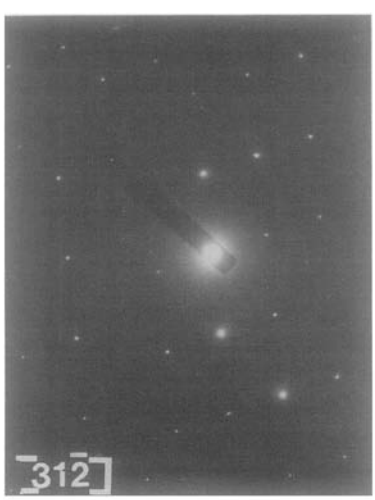

FIG. 14. EDP relative to the tetragonal Gd_2BaCuO_5 compound at 300 K (zone axis [31$\bar{2}$]). The interplanar distances for this structure are: d_{111} = 0.414 and d_{112} = 0.295 nm.

Conclusion

The studies of the macro- and microstructural properties of the new superconductor materials point out some major characteristics. The first is related to the density of defects within the crystals which seem to be strongly varying according to the preparation techniques of each laboratory. In our case one can claim that the crystals present few defects, as clearly shown by all of our electron microscopy observations. The second point is relevant to the chemical analysis of the crystals. As evidenced the whole matrix is defined according to a main com-

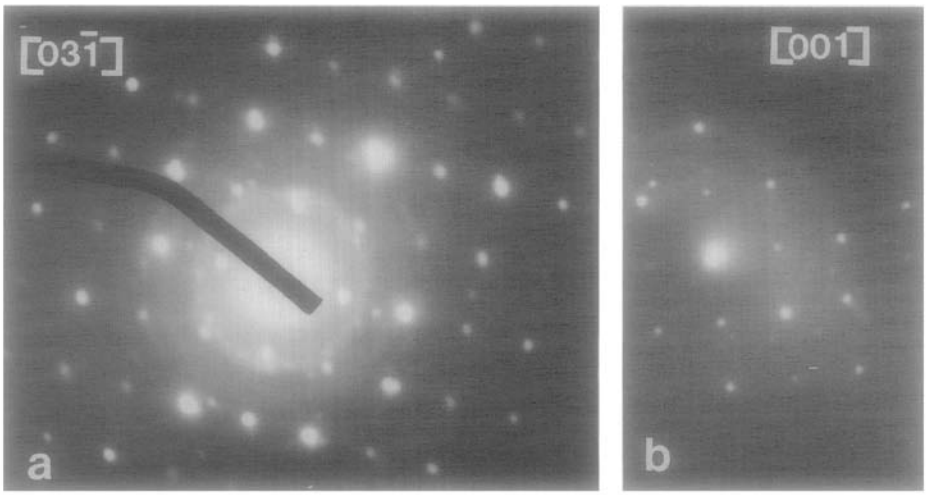

FIG. 15. EDP relative to an unknown compound with tetragonal lattice (from $YBa_2Cu_3O_{7-x}$) (a) after warming from 15 to 300 K, zone axis [03$\bar{1}$]; (b) at 15 K, zone axis [001]. Interplanar distances for this structure are respectively (a) $d_{100} = 0.365$ and $d_{013} = 0.323$ nm and (b) $d_{100,010} = 0.365$ nm.

TABLE II

INTERPLANAR SPACINGS OF THE TETRAGONAL AND PRIMITIVE CUBIC STRUCTURES AND OF THE ORTHORHOMBIC BASIC CELL

Tetragonal $a = 0.365$, $c = 1.985$ nm		Primitive cubic $a = 0.645$ nm		Orthorhombic $a = 0.388$, $b = 0.384$, $c = 1.168$ nm
$h\ k\ l$	d_{hkl}[a]	$h\ k\ l$	d_{hkl}[a]	$h\ k\ l$
0 0 2	0.993			
		1 0 0	0.645	
0 0 4	0.485			
		1 1 0	0.456	
		1 1 1	0.372	~0 1 1
1 0 0	0.365			~0 1 1, 1 0 1
1 0 1	0.359			
0 0 6	0.331			
1 0 3	0.320	2 0 0	0.323	0 1 2
1 0 4	0.292			0 0 4
		2 1 0	0.289	~0 0 4
1 0 5	0.269			1 1 0
		2 1 1	0.263	1 1 1
1 0 6	0.246			1 1 2
1 1 4	0.228	2 2 0	0.228	~1 0 4
1 1 6	0.203	3 1 0	0.204	~1 0 5, 0 1 5
		3 1 1	0.194	0 0 6, 0 2 0
2 0 3	0.176	3 2 0	0.176	1 1 5
2 0 4	0.172	3 2 1	0.172	2 1 0, 0 2 3

[a] The error on calculated d_{hkl} is approximately 2%.

position as $RBa_2Cu_3O_{7-x}$. But microanalyses reveal some fluctuations and the presence of $BaCuO_2$, R_2BaCuO_5, and pseudo-ternary compounds. The first experiments by electron energy loss spectroscopy fitted to a scanning transmission electron microscope reveal, in the nanometer scale, such chemical composition changes (*23*). Finally, some electron diffraction patterns exhibiting complex geometrical configurations show that numerous crystallographic problems are not easy to resolve.

References

1. J. G. BEDNORZ AND K. A. MULLER, *Z. Phys. B* **64,** 189 (1986).
2. C. W. CHU, P. H. HOR, R. L. MENG, L. GAO, Z. J. HUANG, AND Y. Z. WUNG, *Phys. Rev. Lett.* **58,** 405 (1987).
3. A. OURMAZD, J. A. REUTSCHLER, J. C. H. SPENCE, M. O'KEEFFE, R. J. GRAHAM, D. W. JOHNSON, JR., AND W. W. RHODES, *Nature (London)* **327,** 308 (1987).
4. E. A. HEWAT, M. DUPUY, A. BOURRET, J. J. CAPPONI, AND M. MAREZIO, *Nature (London)* **327,** 400 (1987).
5. B. G. HYDE, J. G. THOMPSON, R. L. WITHERS, J. C. FITZGERALD, A. M. STEWART, D. J. M. BE-

VAN, J. S. ANDERSEN, J. BITMEAD, AND M. S. PATERSON, *Nature (London)* **327,** 402 (1987).
6. E. TAKAYAMA, Y. UCHIDA, Y. MATSUI, AND K. KATO, *Japan. J. Appl. Phys.* **26,** L476 (1987).
7. Y. SYONO, M. KIKUCHI, K. OH-ISHI, K. HIRAGA, H. ARAI, Y. MATSUI, N. KOBAYASHI, T. SASAOKA, AND Y. MUTO, *Japan. J. Appl. Phys.* **26,** L498 (1987).
8. A. RELLER, J. G. BEDNORZ, AND K. A. MÜLLER, *Z. Phys. B,* in press.
9. M. HERVIEU, B. DOMENGES, C. MICHEL, G. HEGGER, J. PROVOST, AND B. RAVEAU, *Phys. Rev. B* **36,** 3920 (1987).
10. H. W. ZANBERGEN, G. VAN TENDELOO, T. OKERBE, AND C. AMELINCKX, submitted for publication (1987).
11. R. S. ROTH, K. L. DAVIS AND J. R. DENNIS, *Adv. Ceram. Mat.* (Special Publication on Superconducting Materials) **2**(3B), 303 (1987).
12. L. D. MARKS, J. P. ZHANG, S. J. HWU, AND K. R. POEPPELMEIER, *J. Solid State Chem.* **69,** 189 (1987).
13. M. HERVIEU, B. DOMENGES, C. MICHEL, AND B. RAVEAU, *Europhysics Lett.* **4,** 205 and 211 (1987).
14. Y. KOTANO, K. KIFUNE, I. MUKOUDA, H. KAMIMURA, J. SAKURARI, Y. KOMURA, K. OSHINO, M. SUZUKI, A. MAENO, M. KATO, AND T. FUJITA, *Japan. J. Appl. Phys.* **26,** L394 (1987).
15. D. J. EAGLEMAN, C. J. HUMPHREYS, N. MCN. ALFORD, W. J. CLEGG, M. A. HARMER, AND J. D. BIRCHALL, *Adv. Ceram. Mat.* **2**(3B), 662 (1987); and submitted for publication (1987).
16. S. B. QUADRI, L. E. TOTH, M. OSOFSKY, S. LAWRENCE, D. U. GUBSER, AND S. A. WOLF, *Phys. Rev. B* **35,** 7235 (1987).
17. J. M. TARASCON, L. H. GREENE, W. R. KINNON, AND G. W. HULL, *Phys. Rev. B* **35,** 7115 (1987).
18. M. SALOMÉ, B. RAYNAUD, M. SCHACK, J. CHAUMONT, M.-O. RUAULT, AND H. BERNAS, *J. Phys. E* **18,** 331 (1985).
19. M. GASGNIER AND M.-O. RUAULT, *J. Appl. Phys.* **62,** 4935 (1987).
20. H. NOËL, M. POTEL, P. GOUGEON, AND J. C. LEVET, to be published.
21. P. STOBEL, J. J. CAPPONI, C. CHAILLOUT, M. MAREZIO, AND J. L. THOLENCE, *Nature (London)* **327,** 306 (1987).
22. J. F. MARUCCO, G. NOGUERA, P. GAROCHE, AND G. COLLIN, submitted for publication (1988).
23. C. COLLIEX, *5th Conf. Festkörperanal. Karl-Marx-Stadt, D.D.R.* (June 1987).